The Journal of Nutrition
Biochemical, Molecular, and Genetic Mechanisms

Identification of Selenoprotein H Isoforms and Impact of Selenoprotein H Overexpression on Protein But Not mRNA Levels of 2 Other Selenoproteins in 293T Cells

Lei Cao,[1,2] Tibor Pechan,[3] Sanggil Lee,[4] and Wen-Hsing Cheng[1]

[1]Departments of Food Science, Nutrition, and Health Promotion, Mississippi State University, Mississippi State, MS, USA; [2]Institute of Marine Life Science, Pukyong National University, Busan, Republic of Korea; [3]Institute for Genomics, Biocomputing and Biotechnology, Mississippi State University, Mississippi State, MS, USA; and [4]Department of Food Science and Nutrition, Pukyong National University, Busan, Republic of Korea

ABSTRACT

Background: Selenoprotein H (SELONOH), a member of the thioredoxin-like family proteins, is prioritized to degradation in selenium (Se) insufficiency. Recent studies implicate protective roles of SELENOH in oxidative stress, cellular senescence, and intestinal tumorigenesis. Although the nonselenoprotein H0YE28 is suggested as shortened SELENOH according to genomic and proteomic data repositories, this variant has not been verified biochemically.

Objectives: We sought to identify SELENOH isoforms and explore the impact of Se flux on selenoprotein expression in SELENOH-overexpressing cells.

Methods: A vector expressing a FLAG (the DYKDDDDK sequence) tag on the *N*-terminal end of wild-type SELENOH was constructed and transiently transfected into 293T cells incubated with graded concentrations of Na_2SeO_3 (0–200 nM). Cells were subjected to immunoprecipitation, LC-MS/MS protein analysis, immunoblotting, qRT-PCR, and senescence assays. Data were analyzed by 1-way or 2-way ANOVA.

Results: Results of anti-FLAG immunoblotting showed that FLAG-*SELENOH* transfection increased (3.7-fold; $P < 0.05$) protein levels of the long, but not the short, SELENOH variants in the presence of Na_2SeO_3 (100 nM). By contrast, *SELENOH* mRNA levels were increased by 53-fold upon FLAG-*SELENOH* transfection but were comparable with or without supplemental Se (100 nM). LC-MS/MS analyses of anti-FLAG immunoprecipitates designated both anti-FLAG bands as SELENOH and co-identified three 60S ribosomal and 9 other proteins. Overexpression of FLAG-SELENOH *1*) reduced glutathione peroxidase 1 and thioredoxin reductase 1 expression at the protein rather than the mRNA level in the absence but not presence of supplemental Se (100 nM; $P < 0.05$); *2*) increased mRNA levels of 3 heat shock proteins (*HSP27*, *HSP70-1A*, and *HSP70-1B*; $P < 0.05$); and *3*) reduced senescence induced by H_2O_2 (20 μM, 4 hours; $P < 0.05$).

Conclusions: These cellular studies demonstrate a Se-independent, shortened SELENOH variant and suggest competition of overexpressed FLAG-SELENOH with 2 other selenoproteins for the expression at the protein but not the mRNA level in Se insufficiency. *J Nutr* 2021;151:3329–3338.

Keywords: selenium, selenoprotein H, isoform, proteomics, gene expression

Introduction

Selenium (Se), an essential trace mineral, confers its biological functions mainly through selenoproteins in all 3 domains of life, and the number of selenoproteins in an organism can range from 0 to 59 by species (1–3). Instead of translation termination, the in-frame UGA codon of selenoprotein mRNA is recoded for a selenocysteine (Sec) residue. In eukaryotes, this process requires the *cis*-factor Sec insertion sequence (SECIS) in the 3'-untranslated region and *trans* factors such as Sec-tRNA, Sec-specific elongation factor, a eukaryotic translation initiation factor (eIF4a3), and SECIS-binding protein 2 (4, 5). Se deficiency limits Se amalgamation with Sec-tRNA and stops selenoprotein translation at UGA, resulting in selective degradation through such mechanisms as the cullin-RING E3 ubiquitin ligase 2 (CRL2)–mediated proteasome pathway for truncated selenoproteins (6) and/or nonsense-mediated decay for stalled selenoprotein mRNAs (7, 8). In Se insufficiency, expression of high-hierachy selenoproteins such as thioredoxin reductase 1 (TXNRD1) are prioritized at the expense of low-hierachy ones, including selenoprotein H (SELENOH) and glutathione peroxidase 1 (GPX1) (7, 9).

Manuscript received June 9, 2021. Initial review completed June 16, 2021. Revision accepted August 6, 2021.
First published online September 11, 2021; doi: https://doi.org/10.1093/jn/nxab290.

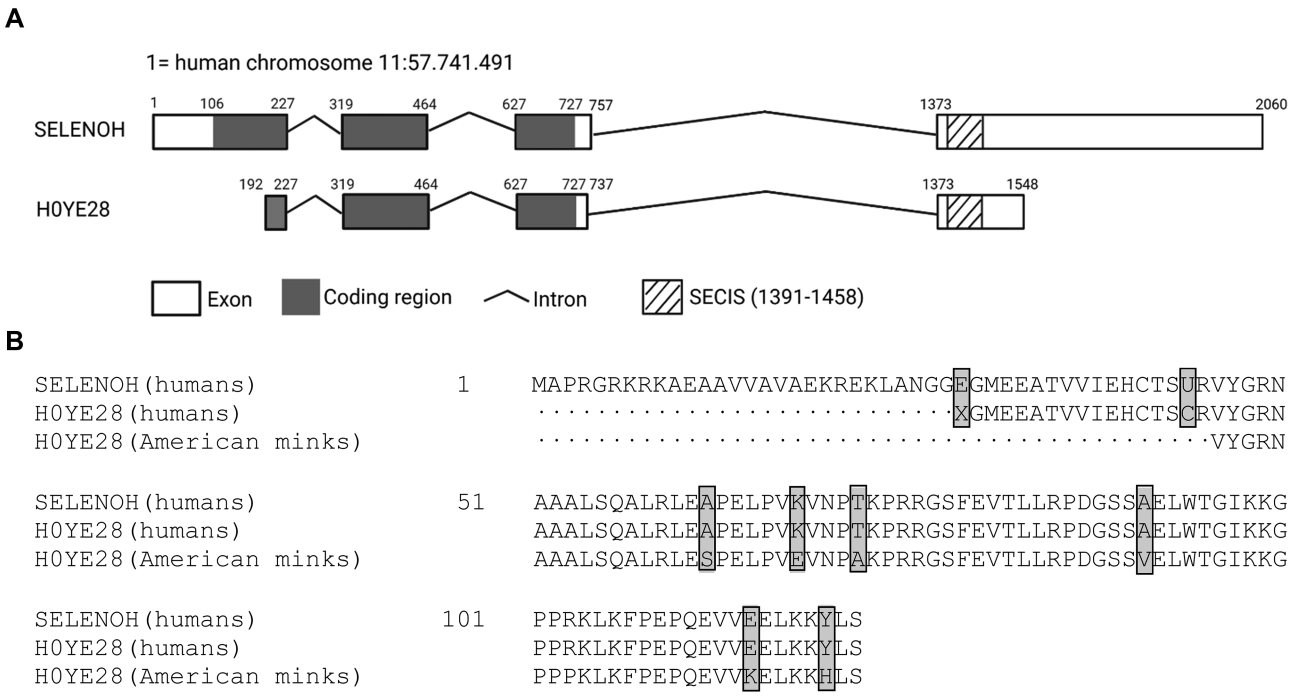

FIGURE 1 A genomic map, splicing variants, and amino acid sequence alignment of SELENOH and the shortened isoforms. (A) Numbers indicate boundaries of exons, coding regions, and/or SECIS in human chromosome 11. Repositories of the full-length SELENOH and H0YE28 in the human genome are at Ensembl (http://useast.ensembl.org/) as ENST00000534355.6 and ENST00000528798.1, respectively. (B) Boxed amino acids differ. Other standard 1-letter amino acid abbreviations apply. Repositories of H0YE28 homologs in humans and American minks (*Neovison vison*) are at https://www.uniprot.org/uniprot/H0YE28 and GenBank (CCP78572.1; https://www.ncbi.nlm.nih.gov/protein/1064634257), respectively. Abbreviations: SECIS, selenocysteine insertion sequence; SELENOH, selenoprotein H; U, selenocysteine; X, unknown.

The third smallest selenoprotein SELENOH (122 amino acids) belongs to the thioredoxin-like family of proteins and carries the conserved CxxU (C, cysteine; x, any amino acid; U, Sec) motif between the 41st and 44th residues (4, 10). *N*-terminal SELENOH contains the RKRK nuclear-targeting and the AT-hook DNA minor groove-binding motifs, corroborating its nucleolar localization and transactivation functions (11, 12). Furthermore, *SELENOH* contains metal response elements in the vicinity of transcription start site (13) and its expression is influenced by exposure to metal or H_2O_2 and by cellular senescence at the mRNA level (13–15). An increasing body of evidence implicates SELENOH in the maintenance of redox homeostasis and as a DNA damage checkpoint together with tumor protein p53 (p53) and the protein kinase ataxia-telangiectasia mutated, the prevention of replicative senescence in primary pulmonary cells, and the mitigation of intestinal tumorigenesis in zebrafish (15, 16); by contrast, SELENOH may promote the differentiation of human colorectal cancer cells (17). Results of other studies link SELENOH to embryogenesis and Se-dependent healthy aging (11, 18–20).

Although bioinformatic repositories reveal H0YE28 as a shortened SELENOH that is missing the first 28 amino acids and has Sec replaced by cysteine in humans [www.uniprot.org/uniprot/H0YE28 (21, 22)] and that is devoid of the first 45 amino acids and lacks the CxxU motif in American minks (GenBank: CCP78572.1; www.ncbi.nlm.nih.gov), these nonselenoprotein variants (**Figure 1**) have not been empirically verified at the protein level. Because untranslated *SELENOH* mRNA could be prone to degradation (7, 9), we also assessed the impacts of *SELENOH* overexpression and the Se status on mRNA and protein expression of SELENOH, GPX1, and TXNRD1 with the use of a vector expressing FLAG (the DYKDDDDK sequence)–tagged full-length SELENOH in 293T cells incubated with or without Na_2SeO_3.

Methods

Construction of SELENOH expression vector

The cloning primers, *CGGAATTCAATGGCTCCCCGCGGGAGG* (forward) and *GCTCTAGATTCAGGATCATGACTGAAGTTTGG* (reverse), were designed to amplify *SELENOH* covering the start codon through SECIS from human neuronal cDNA (ScienCell Research Lab). After purification (QIAquick PCR Purification Kit, Qiagen), the *SELENOH* cDNA cassette was inserted between the EcoRI and XbaI restriction sites of the pFLAG-CMV-4 Expression Vector (Sigma-Aldrich), which contained a 27-nt sequence encoding methionine prior to the DYKDDDDK FLAG tag and an 18-nt insert expressing LAAANS upstream of SELENOH (**Supplemental Figure 1**). The FLAG-*SELENOH* vector was transformed into MAX Efficiency DH5α Competent Cells (Thermo Fisher Scientific) in Lysogeny broth medium

Supported in part by the National Institute of Food and Agriculture (Multistate NE1939, accession no. 1021193, project no. MIS-384060).
Author disclosures: W-HC is a member of the *Journal*'s Editorial Board. All authors report no conflicts of interest.
Supplemental Figures 1–3, Supplemental Tables 1–2, and identified selenoprotein H peptides by LC-MS/MS are available from the "Supplementary data" link in the online posting of the article and from the same link in the online table of contents available on the https://academic.oup.com/jn/.
Address correspondence to W-HC (email: wc523@msstate.edu).
Abbreviations used: CRL2, cullin-RING E3 ubiquitin ligase 2; EV, empty vector; FLAG, the DYKDDDDK sequence; GPX1, glutathione peroxidase 1; HSP, heat shock protein; p53, tumor protein p53; Se, selenium; Sec, selenocysteine; SECIS, selenocysteine insertion sequence; SELENOH, selenoprotein H; TXNRD1, thioredoxin reductase 1.

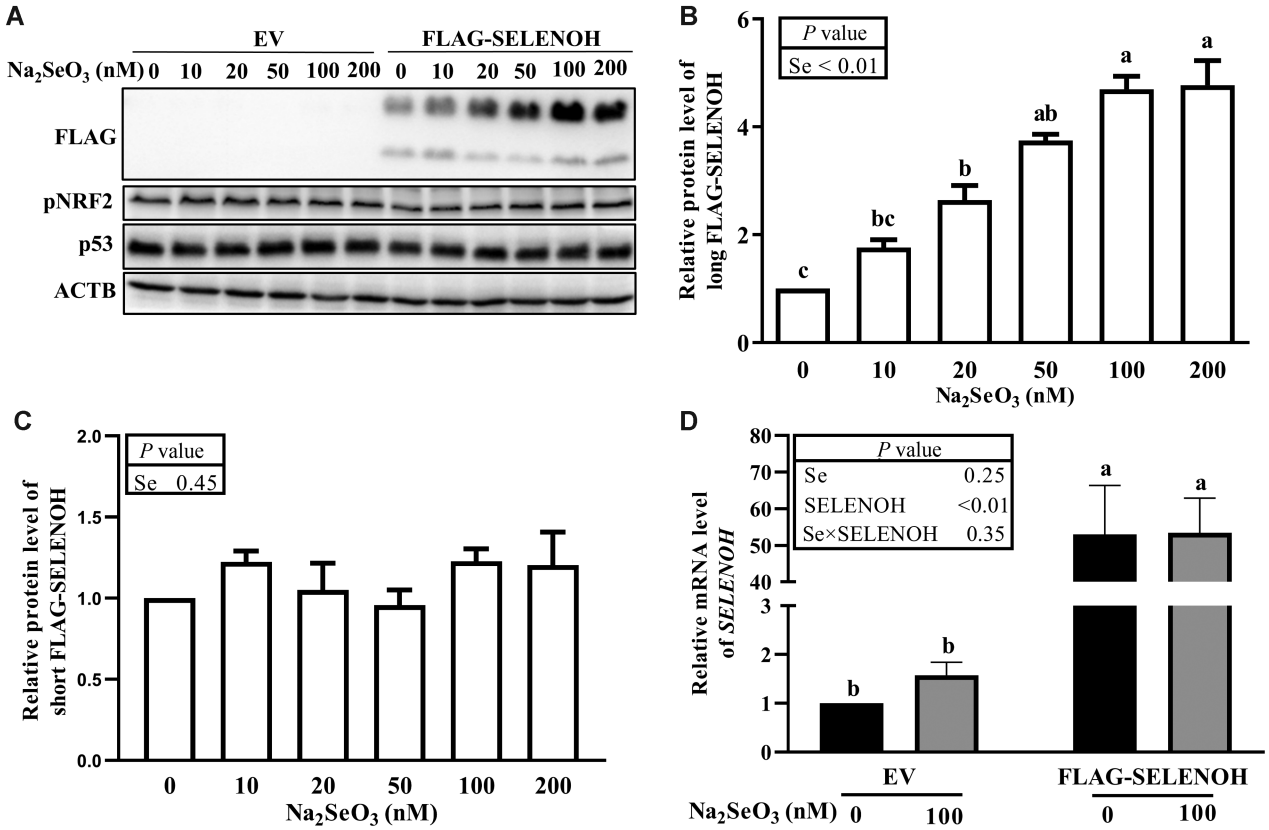

FIGURE 2 (A) Western blotting of long and short FLAG-SELENOH, pNRF2, and p53 and quantification of the (B) long and (C) short FLAG-SELENOH and (D) *SELENOH* mRNA levels in 293T cells transfected with an EV or a FLAG-*SELENOH* vector and incubated with Na_2SeO_3. Values are means ± SEMs ($n = 3$). Data were normalized to ACTB protein or mRNA and calculated relative to the group without Na_2SeO_3. Labeled means without a common letter differ at a P value < 0.05. Abbreviations: ACTB, β-actin; EV, empty vector; FLAG, the DYKDDDDK sequence; pNRF2, phosphorylated nuclear factor (erythroid-derived 2)-like 2; p53, tumor protein p53; Se, selenium; SELENOH, selenoprotein H.

containing ampicillin (100 μg/mL). Amplified vectors were extracted by the PureLink HiPure Plasmid Filter Purification Kit (Thermo Fisher Scientific) and confirmed by DNA sequencing (Eurofins MWG Operon).

Cell culture and transfection

Human 293T and HeLa cells were from American Type Culture Collection and cultured in DMEM containing 10% FBS and 1% penicillin/strepcillin. One day after seeding, cells were transfected (X-tremeGENE 9 DNA Transfection Reagent; Roche) with Opti-MEM-diluted FLAG-*SELENOH* or empty vector (EV), added with Na_2SeO_3 (sodium selenite; 0–200 nM) 6 hours later, and collected 2 days after transfection except senescence assays. Selenite is superior to selenate and selenomethionine for selenoprotein expression in cultured cells (23). The Se concentration was determined using graphite-furnace atomic absorption spectrophotometry with Zeeman-effect background correction (24).

Immunoblotting and qRT-PCR

Cells were sonicated in Laemmli sample buffer (2 × concentrate; Sigma-Aldrich) twice (2 seconds each) and boiled at 95°C for 5 minutes. Room temperature lysates were loaded to separate proteins by SDS-PAGE for immunoblotting as described previously (18), except blocking in 1X Tris-buffered saline with 0.1% Tween-20 detergent and with 5% nonfat milk. Total RNA extraction and qRT-PCR were performed as described previously (19), using iTaq Universal SYBR Green Supermix (Bio-Rad) and the Applied Biosystems 7500 Fast Real-Time PCR System to expand cDNA at 95°C for 30 seconds and subsequently 40 cycles of 95°C for 15 seconds and 60°C for 30 seconds. Antibodies and primers were detailed in **Supplemental Tables 1** and **2**.

Coimmunoprecipitation

FLAG-*SELENOH*-transfected 293T cells were washed with PBS, lysed in a buffer (50 mM Tris-HCl, pH 7.4; 150 mM NaCl; 1 mM EDTA; 1% Triton X-100) containing protease and phosphatase inhibitors (Thermo Fisher Scientific), and centrifuged at 12,000 × g for 10 minutes at 4°C. The supernatants were incubated with anti-mouse Protein A agarose beads at 4°C for 1 hour and spun down at 5000 × g for 2 minutes at 4°C. Next, bead-removed supernatants were incubated with anti-FLAG M2 affinity gel at 4°C overnight and washed with a buffer (50 mM Tris-HCl, pH 7.4; 1 M NaCl) 3 times. Bound proteins were eluted with the 3 × FLAG Peptide (Sigma-Aldrich), followed by 4–20% gradient SDS-PAGE and silver staining to visualize them.

Protein identification by LC–MS/MS

Visible silver-stained bands were excised with a scalpel, digested with trypsin using the in-gel digestion kit (Thermo Fisher Scientific) according to manufacturer instructions, and analyzed by LC-MS/MS as described previously (25). Spectral data were collected by Orbitrap LTQ Velos MS linked with the UltiMate 3000 nano-LC system (Thermo Fisher Scientific). Tryptic digests (2 μg) were loaded on a reversed-phase, fused silica Acclaim PepMap C18 column (diameter, 75 μm; length, 150 mm; Thermo Fisher Scientific). A constant flow rate of 0.3 $\mu L \bullet min^{-1}$ was used to separate and elute peptides via an hour-long linear gradient of acetonitrile (2%–55%, 35 minutes; 95%, 10 minutes; 2%, 15 minutes) in 0.1% formic acid. Peptides were detected by a linear trap mass detector in data-dependent acquisition mode with dynamic exclusion allowed. One MS scan (m/z range: 300–2000) was applied, followed by 7 MS/MS scans for the 7 most intense ions detected in a MS scan using the following parameters: normalized collision energy,

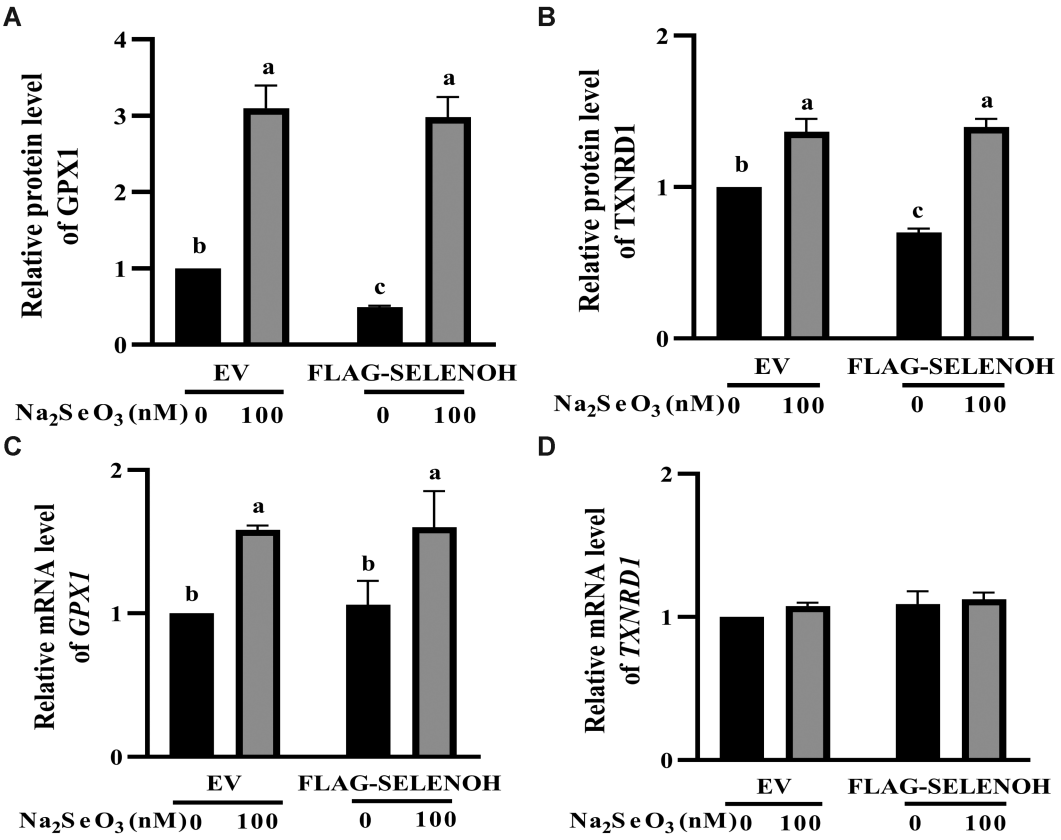

	GPX1	TXNRD1	*GPX1*	*TXNRD1*
Se	<0.01	<0.01	<0.01	0.32
SELENOH	<0.01	0.03	0.07	0.23
Se×SELENOH	<0.01	0.01	0.81	0.69

FIGURE 3 GPX1 and TXNRD1 (A, B) protein and (C, D) mRNA expression in 293T cells transfected with an EV or a FLAG-*SELENOH* vector and incubated with or without Na_2SeO_3. Values are means ± SEMs ($n = 3$). Data were normalized to ACTB protein or mRNA and calculated relative to the EV group in the absence of Na_2SeO_3. Labeled means without a common letter differ at a P value < 0.05. Abbreviations: ACTB, β-actin; EV, empty vector; FLAG, the DYKDDDDK sequence; GPX1, glutathione peroxidase 1; Se, selenium; SELENOH, selenoprotein H; TXNRD1, thioredoxin reductase 1.

35%; automatic gain control, "on"; isolation width (m/z), 2.0; capillary temperature, 230°C; and spray voltage, 1.97 kV.

The .raw files were searched using the SEQUEST algorithm of the Proteome Discoverer 1.1 software (Thermo Fisher Scientific) with the following parameters: lowest and highest charges, +1 and +3, respectively; minimum and maximum precursor mass, 300 and 6000 Da, respectively; enzyme, trypsin; maximum missed cleavages, 2; false discovery rate allowed, <1%; and dynamic modifications of cysteine carbamidomethylation (+57.021), methionine oxidation (+15.995), and methionine dioxidation (+31.990). The spectral data were matched against the *Homo sapiens* protein database (www.ncbi.nlm.nih.gov). The software automatically created a reversed copy as a decoy database to allow for calculation of the false discovery rate.

Senescence assay

One day after the simultaneous vector transfection and Na_2SeO_3 incubation (100 nM), HeLa cells were treated with H_2O_2 (20 μM, 4 hours), maintained in the complete medium for 6 days, and then subjected to senescence-associated β-galactosidase assays as described previously (15).

Statistical analyses

Data were presented as means ± SEMs. The Anderson-Darling test was used to test normality of residuals. For data sets that failed the test, log transformation was conducted prior to ANOVA. Except anti-FLAG immunoblotting by 1-way ANOVA, other results were analyzed by 2-way ANOVA (Se × SELENOH). The level of significance (α) was set at 0.05. Tukey's test was used for multiple mean comparisons. All analyses were conducted using GraphPad Prism 9.0.

Results

Identification of 2 SELENOH isoforms and their differential responses to supplemental Se in 293T cells

Transfection of the FLAG-*SELENOH* vector into Se-supplemented (0–200 nM) 293T cells resulted in the appearance of 2 anti-FLAG immunobands (~17 and 14 kDa; Figure 2A). Because the Se concentration in the basal cell culture medium was 11.4 nM, Se status in these cells was suboptimal (9, 14, 26). In line with this view, GPX1 and TXNRD1 protein levels were 32% and 73%, respectively, of those in Se-supplemented

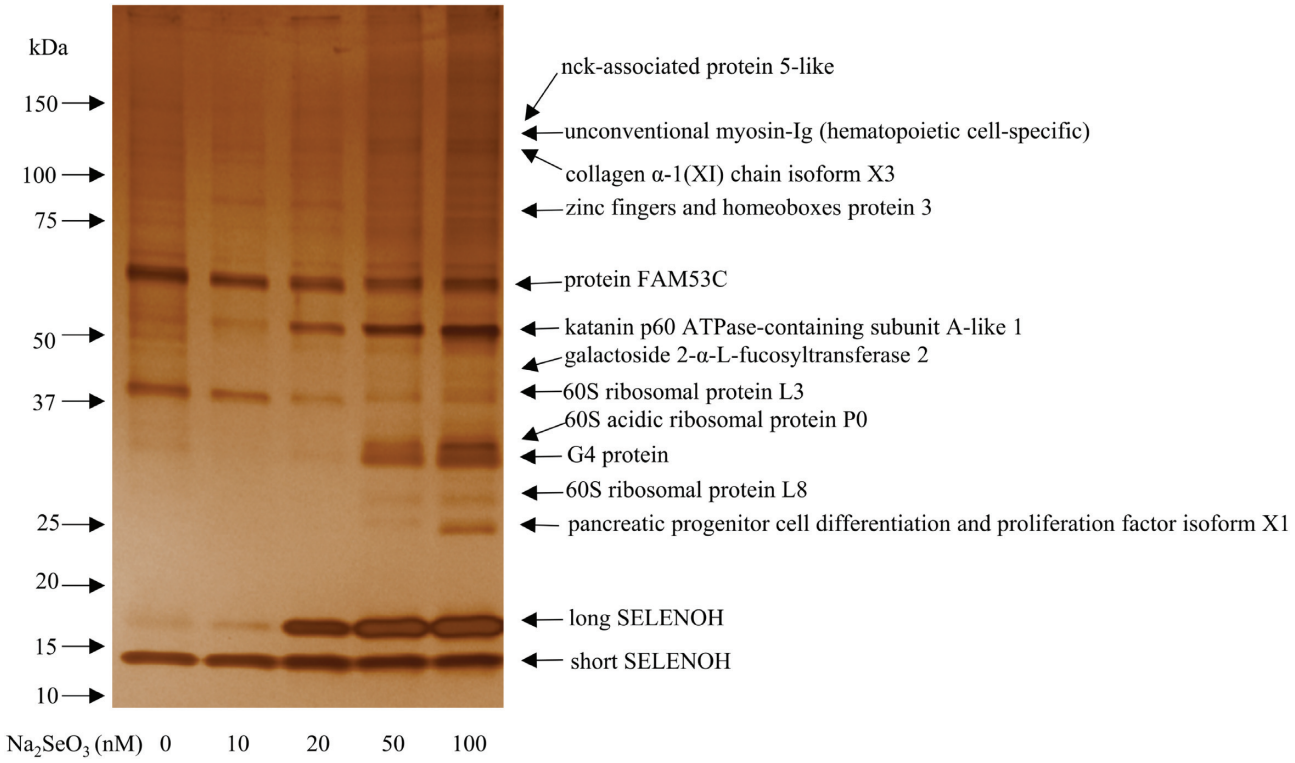

FIGURE 4 Silver-stained bands and LC-MS/MS proteomic identification of proteins in association with anti-FLAG immunoprecipitates being washed with high salt (1 M NaCl) and using whole cell lysates extracted from the FLAG-SELENOH-expressing 293T cells incubated with Na_2SeO_3 (0–100 nM). Arrows indicate positions of the 14 silver-stained and the 9 marker proteins. Abbreviations: FLAG, the DYKDDDDK sequence; SELENOH, selenoprotein H.

cells (100 nM; **Figure 3**A and B). Incubation of these cells with graded concentrations of Na_2SeO_3 (0–200 nM) linearly increased the abundance of the long FLAG-SELENOH ($P < 0.05$), which reached a plateau at 100 nM (Figure 2A and B). By contrast, the level of the short FLAG-SELENOH was independent of Se concentrations (Figure 2A and C). Further proteomic analysis by LC-MS/MS designated both proteins as SELENOH (the last 2 bands; **Figure 4**). Detailed information about identified SELENOH peptides by LC-MS/MS can be found from the Excel file in the online **Supplementary Data**.

Proteins in association with FLAG-SELENOH

Through the anti-FLAG immunoprecipitates prepared from the FLAG-SELENOH-expressing 293T cells incubated with Na_2SeO_3 (100 nM), an LC-MS/MS analysis of the silver-stained SDS-PAGE bands showed that the expected FLAG-containing long and short SELENOH were immunoprecipitated, but that 12 additional proteins were sufficiently coprecipitated. These proteins are named in Figure 4. The immunoprecipitates were washed with a high concentration of NaCl (1 M) to reduce nonspecific protein associations with SELENOH. Consistent with such a stringent condition, levels of at least 5 coprecipitated proteins and the long SELENOH were comparably increased upon incubation of the cells with graded concentrations of Na_2SeO_3 (0–100 nM). By contrast, levels of 60S ribosomal protein L3 and the long SELENOH were inversely associated. Such correlations were not observed in short SELENOH. Coprecipitated proteins >75 kDa were too blurry to assess.

FLAG-SELENOH responds differentially to supplemental Se at protein and mRNA levels in 293T cells

In the FLAG-SELENOH-expressing 293T cells, incubation with Na_2SeO_3 (100 nM) increased the abundance of the long FLAG-SELENOH protein ($P < 0.05$; 3.7-fold) but had no influence on the *SELENOH* mRNA level (Figure 2B and D). Compared with the EV transfection, the FLAG-*SELENOH* transfection increased *SELENOH* mRNA levels by 53- and 34-fold in the absence and presence of supplemental Se, respectively (Figure 2D; $P < 0.05$). Neither FLAG-SELENOH expression nor supplemental Se affected protein levels of phosphorylated nuclear factor (erythroid-derived 2)–like 2 and p53 (Figure 2A; **Supplemental Figure 2**A and B). Overall, only a small portion of the overexpressed *SELENOH* transcripts is translated into FLAG-SELENOH.

Effects of FLAG-SELENOH overexpression and supplemental Se on GPX1 and TXNRD1 expression

Increased expression of a selenoprotein may seize available Se, resulting in reduced expression of other selenoproteins. Consistent with this notion, FLAG-SELENOH overexpression in 293T cells reduced GPX1 and TXNRD1 protein levels by 51% and 30%, respectively ($P < 0.05$), but such suppression was reversed in the presence of Na_2SeO_3 (100 nM; Figure 3A and B). FLAG-*SELENOH* transfection did not influence *GPX1* or *TXNRD1* mRNA levels; supplemental Se (100 nM) increased the *GPX1* (59%; $P < 0.05$) but not the *TXNRD1* mRNA abundance (Figure 3C and D). Supplemental Se and FLAG-*SELENOH* transfection interacted to influence GPX1 and TXNRD1 protein levels. Taken together,

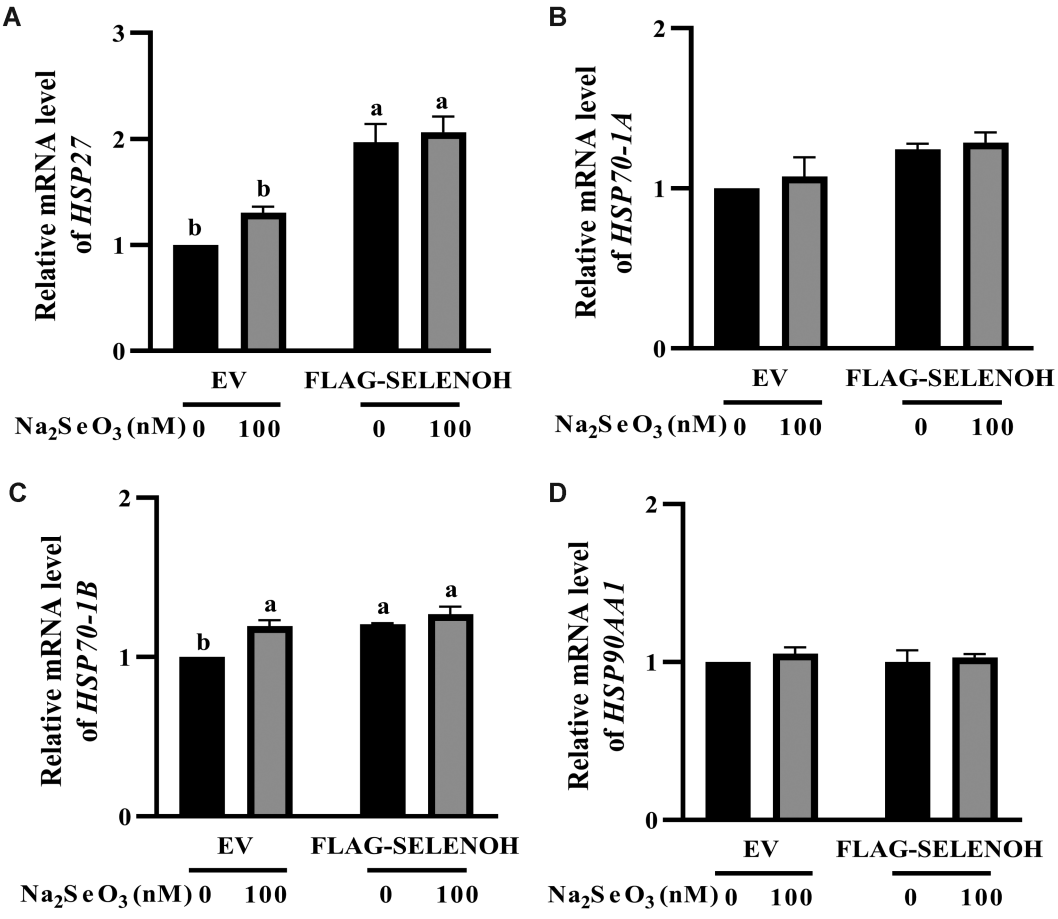

	HSP27	*HSP70-1A*	*HSP70-1B*	*HSP90AA1*
Se	0.13	0.43	<0.01	0.37
SELENOH	<0.01	0.01	<0.01	0.8
Se×SELENOH	0.41	0.84	0.06	0.8

FIGURE 5 (A) *HSP27*, (B) *HSP70-1A*, (C) *HSP70-1B*, and (D) *HSP90AA1* mRNA expression in 293T cells transfected with an EV or a FLAG-*SELENOH* vector and incubated with or without Na_2SeO_3. Values are means ± SEMs ($n = 3$). Data were normalized to *ACTB* mRNA and calculated relative to the EV group in the absence of Na_2SeO_3. Labeled means without a common letter differ at a P value < 0.05. Abbreviations: EV, empty vector; FLAG, the DYKDDDDK sequence; HSP, heat shock protein; Se, selenium; SELENOH, selenoprotein H.

overexpressed FLAG-SELENOH might dominate the Se pool and affect GPX1 and TXNRD1 expression at the level of translation.

Effects of FLAG-SELENOH overexpression on heat shock protein at the mRNA level

Results of chromatin immunoprecipitation analyses show that green fluorescence protein-tagged SELENOH can be in association with heat shock elements (12). Thus, we analyzed mRNA levels of 4 heat shock proteins (HSPs) in 293T cells with FLAG-SELENOH overexpression and/or supplemental Se (100 nM) and found that *1*) FLAG-SELENOH overexpression upregulated *HSP27* (**Figure 5**A), *HSP70-1A* (Figure 5B), and *HSP70-1B* (Figure 5C; $P < 0.05$); and *2*) supplemental Se increased the *HSP70-1B* mRNA level ($P < 0.05$; Figure 5C). The *HSP90AA1* mRNA level was not affected by supplemental Se or FLAG-SELENOH overexpression (Figure 5D). Altogether, the modest transcriptional activation of *HSP* mRNAs by FLAG-SELENOH overexpression may be gene-specific.

FLAG-SELENOH overexpression reduces cellular senescence upon oxidative stress

SELENOH knockdown sensitizes MRC-5 cells to replicative senescence and HeLa cells to oxidant-induced senescence (15). Herein, we showed that H_2O_2-induced senescence (20 μM, 4 hours) in HeLa cells was reduced by FLAG-SELENOH overexpression ($P < 0.05$) and marginally impacted by supplemental Se ($P = 0.06$; **Figure 6**; **Supplemental Figure 3**). For unknown reasons, 293T cells failed to display senescence-associated β-galactosidase expression (data not shown).

Discussion

With the transfection of a FLAG-*SELENOH* vector into 293T cells and biochemical analyses, we report that there are 2 isoforms of the ectopic SELENOH. The short FLAG-SELENOH reacts to an anti-FLAG antibody but fails to show increased protein expression in response to graded levels of supplemental Se, suggesting that the short variant is

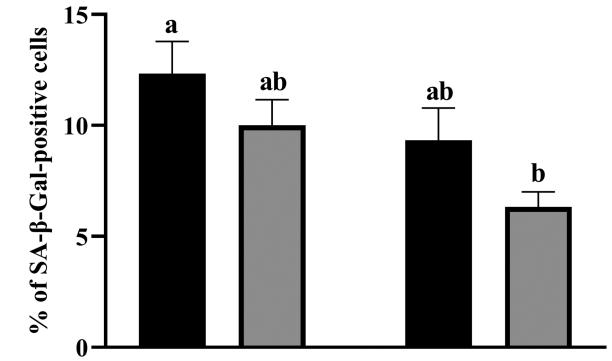

	Se	SELENOH	Se×SELENOH
P value	0.06	0.03	0.79

FIGURE 6 Senescence analysis in HeLa cells transfected with an EV or a FLAG-*SELENOH* vector and incubated with or without Na_2SeO_3, followed by treatment with H_2O_2 (20 μM, 4 hours) and SA-β-Gal staining at day 6. Values are means ± SEMs (n = 3). Representative images are shown in Supplemental Figure 1. Data were calculated as the percentage of the cells positive in SA-β-Gal staining. Labeled means without a common letter differ at a P value < 0.05. Abbreviations: EV, empty vector; FLAG, the DYKDDDDK sequence; SA-β-Gal, senescence-associated β-galactosidase; Se, selenium; SELENOH, selenoprotein H.

not a selenoprotein. By contrast, long FLAG-SELENOH is a selenoprotein. Overexpression of FLAG-SELENOH results in downregulation of GPX1 and TXNRD1 at the protein but not the mRNA level.

It is interesting yet puzzling as to why protein expression of the short FLAG-SELENOH variant is independent of Se. According to public omics repositories (Figure 1B), the *N*-terminally truncated H0YE28 variants in humans (10.4 kDa, 94 residues) and in American minks (8.5 kDa, 77 residues) do not contain Sec and are highly homologous to full-length SELENOH (13.5 kDa, 122 residues). In light of the size difference (~3 kDa) between the long and short FLAG-SELENOH bands based on marker proteins (Figures 2A and 4), it is intuitive to hypothesize the identity of the short FLAG-SELENOH as the 10.4 kDa H0YE28. Nonetheless, the conjecture is not supported by the results of LC-MS/MS, which identify peptides between the 9th to 21st amino acids (KAEAAVVAVAEKR) of SELENOH in the short FLAG-SELENOH (see the Excel file in the **Supplemental Materials**). Despite this, the possibility of the short FLAG-SELENOH being H0YE28 might not be completely excluded considering limitations of our LC-MS/MS analyses of SELENOH, which include *1*) close proximity between these 2 FLAG-SELENOH bands; *2*) efficacy of in-gel digestion of the small-size SELENOH; and *3*) detection of peptides only in the *N*-terminus. Because SELENOH potentially has a total of 19 digestion sites by trypsin, we performed a more efficacious in-solution digestion method with the use of eluted anti-FLAG immunoprecipitates but still matched 85% of all SELENOH peptides to the *N*-terminal sequence of SELENOH (n = 2; data not shown). Altogether, if the short FLAG-SELENOH isoform indeed contains the *N*-terminal sequence of SELENOH, this variant is not H0YE28 and is most likely shortened by alternative splicing in the 3' end of the exon 1, as well as exons 2 and/or 3, of *SELENOH* (Figure 1A). It is warranted to use other approaches such as Edman degradation for *N*-terminal sequencing of the short FLAG-SELENOH.

Whatever the identity, alignments of human SELENOH and H0YE28 genomic DNA (Figure 1A) and amino acids (Figure 1B) revealed some striking attributes. First, human *H0YE28* is completely mapped to *SELENOH* on chromosome 11 despite missing *1*) the first 191 nt of exon 1; *2*) the last 20 nt in the noncoding region of exon 3; and *3*) 74% of exon 4 beginning from the position 90 nt downstream of SECIS. Second, H0YE28 homologs are devoid of the first 28 and 45 residues of SELENOH in humans and American minks, respectively. Third, H0YE28 homologs are highly homologous to SELENOH. Fourth, neither H0YE28 homolog is a selenoprotein; Sec at residue 44 of SELENOH is replaced by cysteine at residue 16 of H0YE28 in humans or is truncated in American minks.

Both human H0YE28 and SELENOH contain a CxxC/U motif and a stretch of eGxFEI(V) sequence characteristic of the thioredoxin-like family proteins (20, 21). H0YE28 might not reside in the nucleus, because it lacks the RKRK nuclear localization sequence located between residues 6 and 9 in SELENOH (Figure 1B) and a GFP-SELENOH with RKRK mutation is known to express in the cytosol (11). Because TXNRD1 with a Sec-to-cysteine mutation displays reduced catalytic activity (27), human H0YE28 is presumably hypomorphic but extends the redox capacity of full-length SELENOH to the cytosol. Likewise, redox functions of the short FLAG-SELENOH we identified might be hampered. Nonetheless, the H0YE28 homolog in American mink lacks both the nuclear localization sequence and the CxxC/U catalytic motif.

How could the protein level of the short FLAG-SELENOH not respond to supplementation with Se? Sec replacement by cysteine occurs in rodent and/or human TXNRD1, TXNRD3, and SELENOP under the condition of a low Sec-tRNA level due to Se deficiency or inhibition of de novo Sec-tRNA synthesis by treatment with thiophosphate, an antagonist of selenophosphate (27–29). However, Sec-tRNA availability does not seem to explain the nonselenoprotein nature of the short FLAG-SELENOH, because the long isoform responds linearly to supplemental Se within the same cells. Although it is pure speculation, the short FLAG-SELENOH might be translated from a configured and shortened mRNA inefficacious for Sec incorporation at UGA or simply devoid of this codon. Consistent with the former notion, Sunde and colleagues showed that a shortened distance between UGA and SECIS could suppress Sec incorporation by as much as 89% in GPX1 (30). In comparison, baseline recoding of in-frame UGA into cysteine has been reported (27–29). Thus, understanding the mechanism by which cysteine is incorporated at in-frame UGA in human H0YE28 might shed light on the nonselenoprotein nature of the short FLAG-SELENOH. Using human H0YE28 as a surrogate, **Figure 7** illustrates conjectures about such an alternative: *1*) loss of the selenoprotein-preferred trimethylguanosine cap in the 5'-untranslated region of the mRNA; *2*) UGA recognition by a yet-to-be-identified cysteine ribonucleoprotein and decoupling it from the machinery for Sec incorporation; and *3*) inhibitory interactions with the SECIS-binding eukaryotic ribosomal protein L30 (31). In line with the latter 2 hypotheses, we identified three 60S ribosomal proteins in the anti-FLAG immunoprecipitates (Figure 4). Although specificity of the co-immunoprecipitation appears high, as evidenced by comparable changes between levels of the long FLAG-SELENOH and the majority of the

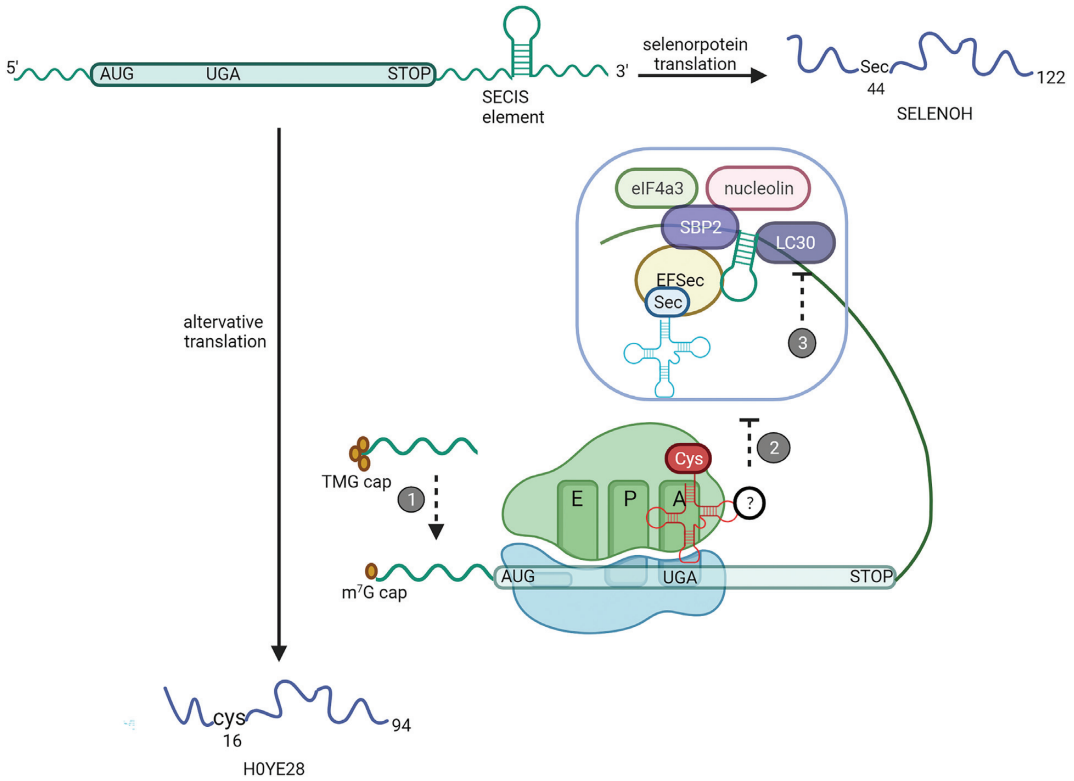

FIGURE 7 Schematic illustration of possible mechanisms underlying the formation of short FLAG-SELENOH using human H0YE28 as a proxy. Illustrations were created with BioRender.com. Abbreviations: Cys, cysteine; EFSec, selenocysteine-specific elongation factor; eIF4a3, eukaryotic translation initiation factor 4a3; LC30, ribosomal L30 protein; FLAG, the DYKDDDDK sequence; m^7G, 7-methylguanosine; SBP2, SECIS-binding protein 2; Sec, selenocysteine; SECIS, selenocysteine insertion sequence; SELENOH, selenoprotein H; TMG, trimethylguanosine.

coprecipitated proteins in a Se dose-dependent manner, immunoblotting is warranted to verify these proteins identified by GC-MS/MS.

In FLAG-*SELENOH*-transfected cells, supplemental Se (100 nM) increases the protein level of the long FLAG-SELENOH by 3.7-fold but has no impact on *SELENOH* mRNA. Although the in-frame UGA codon of *SELENOH* mRNA is located at exon 2 and 136 nt upstream of the exon-exon junction, a preferred target of nonsense-mediated decay in Se insufficiency (7, 14, 32, 33), the 53-fold overexpressed *SELENOH* transcript might exceed the capacity of this pathway. At the protein level, the CRL2-mediated degradation of truncated selenoproteins ending at the otherwise UGA-decoded Sec might not be a mechanism, because this pathway targets a conserved glycine residue at -1 or -2 of the prematurely terminated site (6) and these 2 residues in SELENOH are threonine and serine (Figure 1B). In addition to relatively low Sec-tRNA availability, *trans*-acting factors (34) might ineffectively participate in the translation because the FLAG-*SELENOH* vector lacks the entire 5'-untranslated region and the majority of 3'-untranslated region downstream of SECIS (Figure 1A; Supplemental Figure 1). Despite pure speculation, multiple proteins collectively known as a "ribosome quality control complex" may also be recruited to stalled 60S ribosome and ubiquitylate nascent polypeptide cotranslationally (35), resulting in degradation of the shortened FLAG-SELENOH at UGA.

Expression of high-hierarchy selenoproteins such as TXNRD1 is prioritized when the Se status is suboptimal (7, 14, 33). Likewise, in the absence of supplemental Se, the 53-fold overexpressed *SELENOH* transcript may dominate the Se flux for prioritized protein expression at the expense of other selenoproteins. This may explain the observations of reduced protein but comparable mRNA levels of GPX1 and TXNRD1 in FLAG-*SELENOH*-transfected 293T cells without supplemental Se. Nonetheless, it remains possible that endogenous SELENOH or the short FLAG-SELENOH might influence the Se flux in FLAG-*SELENOH*-transfected cells.

According to studies in cells with *SELENOH* knockdown, *Gpx1* knockout, and TXNRD1 inhibition (15, 36, 37), these selenoproteins carrying oxidoreductase activity may play overlapping roles in the protection against oxidative stress and senescence. Herein, we show that FLAG-SELENOH overexpression and supplemental Se are beneficial to protect against H_2O_2-induced senescence. Although incubation of cells with Se compounds at high doses induces oxidative stress and senescence (38), Se concentrations ranging from 10 to 100 nM are considered physiological and largely improve Se status for selenoprotein expression. While p53 and phosphorylated nuclear factor (erythroid-derived 2)–like 2 are activated by SELENOH deficiencies in zebrafish and human cells (15, 16, 39), they are not influenced by FLAG-*SELENOH* transfection in 293T cells with supplemental Se or in murine neuron cells (40), suggesting that our cells are not in a stressed or toxic status following the transfection.

Our results implicate SELENOH in the upregulation of certain HSP mRNAs, which are known to be induced by heat or oxidative stress but degraded during mammalian aging (41, 42). Expression of HSP70F is positively correlated with longevity in *Drosophila* (43) and *Caenorhabditis elegans* (44), and HSP27 may protect against apoptosis in Huntington's disease (45). Interestingly, Se supplementation is linked to induction of HSPs

in chicken splenic lymphocytes and the lenses from the pups of Wistar rats (46, 47). It is of future interest to test whether upregulation of *HSP27*, *HSP70-1A*, and *HSP70-1B* by FLAG-SELENOH overexpression confers protection against stress-induced senescence.

Altogether, our findings provide biochemical evidence to corroborate the existence of a shortened, Se-independent SELENOH. When overexpressed, the long SELENOH isoform may compete with other selenoproteins for Se incorporation during translation. Although it is unknown whether the short SELENOH isoform exists endogenously and exerts physiological functions or how it is shortened, a CxxU-to-CxxC SELENOH mutant remains capable of decomposing H_2O_2 (11). We speculate that SELENOH isoforms may exhibit functions to a various extent and/or be present in different subcellular localization to exert distinctive and common functions in redox regulation, ribosome biogenesis, and/or transactivation of selective genes.

Acknowledgments

The author's responsibilities were as follows—LC and W-HC: designed the research; LC and TP: conducted the experiments; LC, TP, SL and W-HC: analyzed the data; LC, TP and W-HC: wrote the manuscript; W-HC: had primary responsibility for the final content; and all authors: analyzed the data and read and approved the final manuscript.

References

1. Gobler CJ, Lobanov AV, Tang YZ, Turanov AA, Zhang Y, Doblin M, Taylor GT, Sanudo-Wilhelmy SA, Grigoriev IV, Gladyshev VN. The central role of selenium in the biochemistry and ecology of the harmful pelagophyte, *Aureococcus anophagefferens*. ISME J 2013;7:1333–43.
2. Mariotti M, Salinas G, Gabaldon T, Gladyshev VN. Utilization of selenocysteine in early-branching fungal phyla. Nat Microbiol 2019;4:759–65.
3. Kryukov GV, Castellano S, Novoselov SV, Lobanov AV, Zehtab O, Guigó R, Gladyshev VN. Characterization of mammalian selenoproteomes. Science 2003;300:1439–43.
4. Labunskyy VM, Hatfield DL, Gladyshev VN. Selenoproteins: molecular pathways and physiological roles. Physiol Rev 2014;94:739–77.
5. Xu XM, Carlson BA, Mix H, Zhang Y, Saira K, Glass RS, Berry MJ, Gladyshev VN, Hatfield DL. Biosynthesis of selenocysteine on its tRNA in eukaryotes. PLoS Biol 2007;5:e4.
6. Lin H-C, Ho S-C, Chen Y-Y, Khoo K-H, Hsu P-H, Yen H-CS. CRL2 aids elimination of truncated selenoproteins produced by failed UGA/Sec decoding. Science 2015;349:91–5.
7. Seyedali A, Berry MJ. Nonsense-mediated decay factors are involved in the regulation of selenoprotein mRNA levels during selenium deficiency. RNA 2014;20:1248–56.
8. Sun X, Li X, Moriarty PM, Henics T, LaDuca JP, Maquat LE. Nonsense-mediated decay of mRNA for the selenoprotein phospholipid hydroperoxide glutathione peroxidase is detectable in cultured cells but masked or inhibited in rat tissues. Mol Biol Cell 2001;12:1009–17.
9. Sunde RA, Raines AM. Selenium regulation of the selenoprotein and nonselenoprotein transcriptomes in rodents. Adv Nutr 2011;2:138–50.
10. Dikiy A, Novoselov SV, Fomenko DE, Sengupta A, Carlson BA, Cerny RL, Ginalski K, Grishin NV, Hatfield DL, Gladyshev VN. SelT, SelW, SelH, and Rdx12: genomics and molecular insights into the functions of selenoproteins of a novel thioredoxin-like family. Biochemistry 2007;46:6871–82.
11. Novoselov SV, Kryukov GV, Xu X-M, Carlson BA, Hatfield DL, Gladyshev VN. Selenoprotein H is a nucleolar thioredoxin-like protein with a unique expression pattern. J Biol Chem 2007;282:11960–8.
12. Panee J, Stoytcheva ZR, Liu W, Berry MJ. Selenoprotein H is a redox-sensing high mobility group family DNA-binding protein that up-regulates genes involved in glutathione synthesis and phase II detoxification. J Biol Chem 2007;282:23759–65.
13. Stoytcheva ZR, Vladimirov V, Douet V, Stoychev I, Berry MJ. Metal transcription factor-1 regulation via MREs in the transcribed regions of selenoprotein H and other metal-responsive genes. Biochim Biophys Acta 2010;1800:416–24.
14. Legrain Y, Touat-Hamici Z, Chavatte L. Interplay between selenium levels, selenoprotein expression, and replicative senescence in WI-38 human fibroblasts. J Biol Chem 2014;289:6299–310.
15. Wu RT, Cao L, Chen BP, Cheng W-H. Selenoprotein H suppresses cellular senescence through genome maintenance and redox regulation. J Biol Chem 2014;289:34378–88.
16. Cox AG, Tsomides A, Kim AJ, Saunders D, Hwang KL, Evason KJ, Heidel J, Brown KK, Yuan M, Lien EC. Selenoprotein H is an essential regulator of redox homeostasis that cooperates with p53 in development and tumorigenesis. Proc Natl Acad Sci 2016;113:E5562–71.
17. Bertz M, Kuhn K, Koeberle SC, Muller MF, Hoelzer D, Thies K, Deubel S, Thierbach R, Kipp AP. Selenoprotein H controls cell cycle progression and proliferation of human colorectal cancer cells. Free Radic Biol Med 2018;127:98–107.
18. Cao L, Zhang L, Zeng H, Wu RT, Wu TL, Cheng WH. Analyses of selenotranscriptomes and selenium concentrations in response to dietary selenium deficiency and age reveal common and distinct patterns by tissue and sex in telomere-dysfunctional mice. J Nutr 2017;147:1858–66.
19. Wu RT, Cao L, Mattson E, Witwer KW, Cao J, Zeng H, He X, Combs GF, Jr., Cheng WH. Opposing impacts on healthspan and longevity by limiting dietary selenium in telomere dysfunctional mice. Aging Cell 2017;16:125–35.
20. Zhang L, Zeng H, Cheng W-H. Beneficial and paradoxical roles of selenium at nutritional levels of intake in healthspan and longevity. Free Radic Biol Med 2018;127:3–13.
21. Taylor TD, Noguchi H, Totoki Y, Toyoda A, Kuroki Y, Dewar K, Lloyd C, Itoh T, Takeda T, Kim DW, et al. Human chromosome 11 DNA sequence and analysis including novel gene identification. Nature 2006;440:497–500.
22. Cuadrado E, van den Biggelaar M, de Kivit S, Chen YY, Slot M, Doubal I, Meijer A, van Lier RAW, Borst J, Amsen D. Proteomic analyses of human regulatory T cells reveal adaptations in signaling pathways that protect cellular identity. Immunity 2018;48:1046–59.
23. Hoefig CS, Renko K, Köhrle J, Birringer M, Schomburg L. Comparison of different selenocompounds with respect to nutritional value vs. toxicity using liver cells in culture. J Nutr Biochem 2011;22:945–55.
24. Davis CD, Zeng H, Finley JW. Selenium-enriched broccoli decreases intestinal tumorigenesis in multiple intestinal neoplasia mice. J Nutr 2002;132:307–9.
25. Takáč T, Vadovič P, Pechan T, Luptovčiak I, Šamajová O, Šamaj J. Comparative proteomic study of Arabidopsis mutants mpk4 and mpk6. Sci Rep 2016;6:28306.
26. Kipp A, Banning A, van Schothorst EM, Meplan C, Schomburg L, Evelo C, Coort S, Gaj S, Keijer J, Hesketh J. Four selenoproteins, protein biosynthesis, and Wnt signalling are particularly sensitive to limited selenium intake in mouse colon. Mol Nutr Food Res 2009;53:1561–72.
27. Lu J, Zhong L, Lonn ME, Burk RF, Hill KE, Holmgren A. Penultimate selenocysteine residue replaced by cysteine in thioredoxin reductase from selenium-deficient rat liver. FASEB J 2009;23:2394–402.
28. Turanov AA, Everley RA, Hybsier S, Renko K, Schomburg L, Gygi SP, Hatfield DL, Gladyshev VN. Regulation of selenocysteine content of human selenoprotein P by dietary selenium and insertion of cysteine in place of selenocysteine. PLoS One 2015;10:e0140353.
29. Xu X-M, Turanov AA, Carlson BA, Yoo M-H, Everley RA, Nandakumar R, Sorokina I, Gygi SP, Gladyshev VN, Hatfield DL. Targeted insertion of cysteine by decoding UGA codons with mammalian selenocysteine machinery. Proc Natl Acad Sci 2010;107:21430–4.
30. Wen W, Weiss SL, Sunde RA. UGA codon position affects the efficiency of selenocysteine incorporation into glutathione peroxidase-1. J Biol Chem 1998;273:28533–41.
31. Howard MT, Copeland PR. New directions for understanding the codon redefinition required for selenocysteine incorporation. Biol Trace Elem Res 2019;192:18–25.
32. Popp MW-L, Maquat LE. Organizing principles of mammalian nonsense-mediated mRNA decay. Annu Rev Genet 2013;47:139–65.

33. Sunde R, Raines A, Barnes K, Evenson J. Selenium status highly regulates selenoprotein mRNA levels for only a subset of the selenoproteins in the selenoproteome. Biosci Rep 2009;29:329–38.
34. Wilkie GS, Dickson KS, Gray NK. Regulation of mRNA translation by 5′- and 3′-UTR-binding factors. Trends Biochem Sci 2003;28: 182–8.
35. Brandman O, Stewart-Ornstein J, Wong D, Larson A, Williams CC, Li G-W, Zhou S, King D, Shen PS, Weibezahn J, et al. A ribosome-bound quality control complex triggers degradation of nascent peptides and signals translation stress. Cell 2012;151:1042–54.
36. de Haan JB, Bladier C, Lotfi-Miri M, Taylor J, Hutchinson P, Crack PJ, Hertzog P, Kola I. Fibroblasts derived from Gpx1 knockout mice display senescent-like features and are susceptible to H_2O_2-mediated cell death. Free Radic Biol Med 2004;36:53–64.
37. Volonte D, Galbiati F. Inhibition of thioredoxin reductase 1 by caveolin 1 promotes stress-induced premature senescence. EMBO Rep 2009;10:1334–40.
38. Wu M, Kang MM, Schoene NW, Cheng WH. Selenium compounds activate early barriers of tumorigenesis. J Biol Chem 2010;285: 12055–62.
39. Lee J-S, Surh Y-J. Nrf2 as a novel molecular target for chemoprevention. Cancer Lett 2005;224:171–84.
40. Mendelev N, Witherspoon S, Li PA. Overexpression of human selenoprotein H in neuronal cells ameliorates ultraviolet irradiation-induced damage by modulating cell signaling pathways. Exp Neurol 2009;220:328–34.
41. Kregel KC. Heat shock proteins: modifying factors in physiological stress responses and acquired thermotolerance. J Appl Physiol 2002;92:2177–86.
42. Calderwood SK, Murshid A, Prince T. The shock of aging: molecular chaperones and the heat shock response in longevity and aging–a mini-review. Gerontology 2009;55:550–8.
43. Kurapati R, Passananti HB, Rose MR, Tower J. Increased hsp22 RNA levels in *Drosophila* lines genetically selected for increased longevity. J Gerontol A Biol Sci Med Sci 2000;55:B552–9.
44. Yokoyama K, Fukumoto K, Murakami T, Harada S-i, Hosono R, Wadhwa R, Mitsui Y, Ohkuma S. Extended longevity of *Caenorhabditis elegans* by knocking in extra copies of hsp70F, a homolog of mot-2 (mortalin)/mthsp70/Grp75. FEBS Lett 2002;516: 53–7.
45. Wyttenbach A, Sauvageot O, Carmichael J, Diaz-Latoud C, Arrigo A-P, Rubinsztein DC. Heat shock protein 27 prevents cellular polyglutamine toxicity and suppresses the increase of reactive oxygen species caused by huntingtin. Hum Mol Genet 2002;11:1137–51.
46. Manikandan R, Beulaja M, Thiagarajan R, Arumugam M. Effect of curcumin on the modulation of αA- and αB-crystallin and heat shock protein 70 in selenium-induced cataractogenesis in Wistar rat pups. Mol Vis 2011;17:388–94.
47. Chen X, Zhu Y-H, Cheng X-Y, Zhang Z-W, Xu S-W. The protection of selenium against cadmium-induced cytotoxicity via the heat shock protein pathway in chicken splenic lymphocytes. Molecules 2012;17:14565–72.